ACS OMEGA

http://pubs.acs.org/journal/acsodf

Article

Pulse Radiolysis and Transient Absorption of Aqueous Cr(VI) Solutions up to 325 °C

Jacy K. Conrad,* Aliaksandra Lisouskaya, and David M. Bartels*

Cite This: *ACS Omega* 2022, 7, 39071−39077

Read Online

ACCESS | Metrics & More | Article Recommendations | Supporting Information

ABSTRACT: Pulse radiolysis with a custom multichannel detection system has been used to measure the kinetics of the radiation chemistry reactions of aqueous solutions of chromium(VI) to 325 °C for the first time. Kinetic traces were measured simultaneously over a range of wavelengths and fit to obtain the associated high-temperature rate coefficients and Arrhenius parameters for the reactions of Cr(VI) + e_{aq}^-, Cr(VI) + H•, and Cr(V) + •OH. These kinetic parameters can be used to predict the behavior of toxic Cr(VI) in models of aqueous systems for applications in nuclear technology, industrial wastewater treatment, and chemical dosimetry.

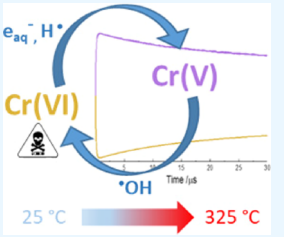

1. INTRODUCTION

Understanding the ionizing radiation-induced speciation of chromium ions in aqueous solution over a range of temperatures is useful for several applications. First, chromium is found in the coolant systems of industrial processes as it is a corrosion product and primary leachate from various metal alloys, including stainless steels.[1] Aqueous chromates found in industrial wastewaters are highly mobile, and the Cr(VI) oxidation state is very toxic, making it a significant environmental concern.[1] In particular, in nuclear technologies, circulating coolant systems experience intense, multicomponent radiation fields and temperatures up to 315 °C.[2] Understanding the speciation of chromates under extreme conditions is essential for operating these systems and safely disposing of their waste products. Ionizing radiation has also been proposed as an efficient method to reduce toxic Cr(VI) to less harmful and less soluble Cr(III) prior to its release into the environment,[3,4] but more data and accurate models of these radiation chemistry reactions are required before this procedure can be efficiently implemented. In addition, potassium dichromate systems have been considered for use as chemical dosimeters because changes in absorbed dose, dose rate, and the amount of oxygen during irradiation present little effect on the observed reduction yield, and thus, the dosimeter has a stable response.[5−8] In order to use potassium dichromate as a benchmark system, however, the radiation-induced behavior of aqueous chromium ions must be well understood and studied over a variety of experimental conditions.

When a dilute aqueous solution interacts with ionizing radiation, the radiolysis of the water solvent produces a suite of highly reactive oxidizing and reducing species:

$$H_2O \rightsquigarrow 2.73\ e_{aq}^- + 2.79\ {}^\bullet OH + 0.60\ H^\bullet + 0.45\ H_2 + 0.7\ H_2O_2 + 2.73\ H_{aq}^+ \quad (1)$$

where the coefficients represent the room-temperature escape yields (G values) of the species in units of molecules/100 eV.[9] The reactive species from water radiolysis can undergo subsequent reactions with many of the aqueous solution matrix chemicals present to generate secondary radiolysis products,[10] or they can react with any nearby solutes, such as aqueous chromium ions. Chromium ions are present in dilute aqueous solutions of Cr(VI) in the form of chromic acid:[11−14]

$$H_2CrO_4 \rightleftharpoons HCrO_4^- + H^+,\ pK_{1a} = -1.0 \text{ to } 1.6 \text{ at } 25\ ^\circ C \quad (2)$$

$$HCrO_4^- \rightleftharpoons CrO_4^{2-} + H^+,\ pK_{2a} = 6.472 \text{ at } 25\ ^\circ C \quad (3)$$

where the ionization constants and their temperature and ionic strength dependencies can be derived from fits to thermodynamic data.[11,12,14−18] The polynuclear dimeric dichromate ion, $Cr_2O_7^{2-}$, also exists at higher concentrations than those studied in this work, and it becomes the dominant form of Cr(VI) below pH 5 at [Cr(VI)] > 7 mM.[11,14] Some reactions between the radiolysis products of water and these chromium ions have been studied in the past,[5−7,19−26] but the pH and exact Cr speciation in these solutions are rarely reported, and the temperature dependance of the reported rate coefficients are largely unknown. In addition, most of the literature does not specify the uncertainties or any ionic strength corrections that may have been employed, making comparison of these values difficult. In the present study, we use pulse electron radiolysis up to 325 °C to measure the rate coefficients and Arrhenius

Received: July 29, 2022
Accepted: October 7, 2022
Published: October 21, 2022

parameters for major reactions essential for understanding and modeling the behavior of aqueous Cr(VI) under irradiation.

2. EXPERIMENTAL SECTION

$K_2Cr_2O_7$ (ReagentPlus, >99.5%), $HClO_4$ (70%, 99.999% trace metal basis), and methanol (>99%) were purchased from Millipore Sigma. KSCN (98%) was purchased from Alfa Aesar. Standard 1 M NaOH solution was obtained from LabChem. All chromium solution concentrations were determined using UV−visible spectroscopy at λ = 350 nm with an acidic Cr(VI) extinction coefficient: ε = 1485 ± 5 M^{-1} cm^{-1}, measured in this work. All solutions were prepared using deionized water with 18 MΩ cm resistivity and <10 ppb total organic carbon obtained from a Serv-A-Pure Co. cartridge system.

Time-resolved electron pulse radiolysis experiments were performed at the Notre Dame Radiation Laboratory (NDRL) using nanosecond electron pulses from an 8 MeV linear accelerator (LINAC). The transient absorptions of different species were followed for the various chemical reactions studied using a multichannel detection system.[27] A 1000 W xenon lamp probe light is dispersed via an Acton SP2300 f/3.9 30 cm imaging spectrograph onto an array of twenty-four 50 cm length UV-transmitting fiber optic bundles. The bundles each terminate in a photodiode directly coupled to a two-stage operational amplifier assembly connected to digital oscilloscopes for data collection. This bespoke setup allows for simultaneous measurement of a full spectrum with resolutions of approximately 6, 12, or 24 nm per channel depending on the grating selected. This work used the grating with 12 nm per channel resolution over the wavelength range of ∼250−550 nm.

The transient absorption measurements were made using two different optical cells. The experiments were performed up to 325 °C using a custom-built high-temperature high-pressure titanium cell with sapphire windows and an effective optical pathlength of 2.0 cm, similar to the Hastelloy cell described previously.[28] The decay of the e_{aq}^- at 25 °C in pure, deaerated water at 720 nm was used as a dosimeter for this cell. Two high-pressure ISCO 260D syringe pumps (Teledyne Isco Inc.) were used to set the experimental pressure to 19.5 ± 0.3 MPa. One pump was filled with a Cr stock solution and the other with water at an equivalent pH such that the solutions could be mixed in an appropriate ratio at a tee connection and supplied to the cell. The mixed solutions were flowed through a preheater coil, into the heated titanium cell located at the end of the electron beamline and out to waste via a backpressure regulator. The Cr(VI) + $H^\bullet$ at pH 1.1 kinetic study was performed up to 70 °C at atmospheric pressure in a fused silica cell with an optical pathlength of 1 cm. Solutions entering this cell were heated by flowing through a preheater which consisted of a glass coil containing a circulating heated mixture of glycol and water from a temperature bath. The thiocyanate dosimeter was used to determine the absorbed dose in the glass cell (λ_{max} = 475 nm; G_ε = 5.2 × 10^{-4} m^2 J^{-1}).[7] The following solution conditions were used to isolate specific radical species for study:

- Hydrated electron (e_{aq}^-). Direct transient decay kinetics of e_{aq}^- were observed at 532 nm using N_2- or Ar-saturated aqueous solutions with pH adjusted by concentrated $HClO_4$ or NaOH.
- Hydrogen atom ($H^\bullet$). The bleach kinetics of Cr(VI) were monitored at 348 nm in N_2-saturated aqueous solutions with pH adjusted to 1.1, 4.0, and 5.5 using $HClO_4$.
- Hydroxyl radical ($^\bullet OH$). For Cr(V), the postbleach recovery of Cr(VI) from its reactions with e_{aq}^- and $H^\bullet$ in N_2- or Ar-saturated aqueous solutions was observed at 348 nm.

Fitted kinetic traces were an average of 2−4 identical experiments, each of which consisted of six individual measurements. At each temperature, the transient absorption was recorded at a minimum of five Cr concentrations and two doses to check for second-order kinetic effects. Depending on the reaction studied, second-order rate coefficients (k) were either derived from pseudo-first-order exponential fits (k') to raw kinetic data by plotting k' against the reactant concentration weighted by the inverse squares of the experimental uncertainties, or they were calculated directly by fitting the observed optical absorbance with coupled ordinary differential equations representing the suite of chemical reactions relevant to the system. Quoted errors for the presented second-order reaction rate coefficients are a combination of measurement precision, sample concentration errors, and uncertainties in the fitted parameters. The IGOR Pro software package from Wavemetrics Inc. was used to fit the data. The change in absorbed radiation due to the decrease in the density of water with the increasing temperature was accounted for in fitting the experimental data.

The observed rates for the reactions between the aqueous chromate species and e_{aq}^- are influenced by ionic strength. These rates have all been corrected for this effect by the Debye−Brønsted equation:

$$\log(k_i) = \log(k_0) + 2AZ_1Z_2I^{0.5} \quad (4)$$

where k_i and k_0 are the rate constants at ionic strength i and zero, respectively, Z_1 and Z_2 are charges of reactants 1 and 2, respectively, I is the ionic strength in mol L^{-1}, and A is the temperature-dependent Debye−Hückel constant calculated using

$$A = \frac{e^3(2000N_A)^{1/2}}{2.303(8\pi)(\varepsilon_0\varepsilon k_B T)^{3/2}} \quad (5)$$

where e is the electron charge, N_A is Avogadro's number, ε_0 is the vacuum permittivity, ε is the solvent dielectric constant, k_B is the Boltzmann constant, T is the temperature in K, and a factor of 1000 is used to convert between the moles per liter and moles per cubic meter concentration basis.

3. RESULTS AND DISCUSSION

3.1. Multichannel Detection System. The multichannel detection system used in this work proved to be very powerful, as the rate coefficients for Cr(VI) + e_{aq}^-, Cr(VI) + $H^\bullet$, and Cr(V) + $^\bullet OH$ could all be obtained from a single experiment at an appropriate pH by choosing a suitable wavelength for fitting the respective rate coefficients. Figure 1 shows a "waterfall" plot of the range of wavelengths measured simultaneously for a 49.5 μM $K_2Cr_2O_7$ solution at pH 9.8 and 25 °C with a 15 ns electron pulse of 26.8 Gy, alongside a plot showing the absorbance maxima of this solution when unirradiated over the same wavelength range. One can see that at wavelengths nearest the absorption maxima of CrO_4^{2-} (∼279 and 373 nm), the kinetic traces show an initial bleach up to 10 μs and subsequent recovery of the CrO_4^{2-} absorbance from the reactions of Cr(VI) + e_{aq}^-, Cr(VI) + $H^\bullet$, and Cr(V) +

https://doi.org/10.1021/acsomega.2c04807
ACS Omega 2022, 7, 39071−39077

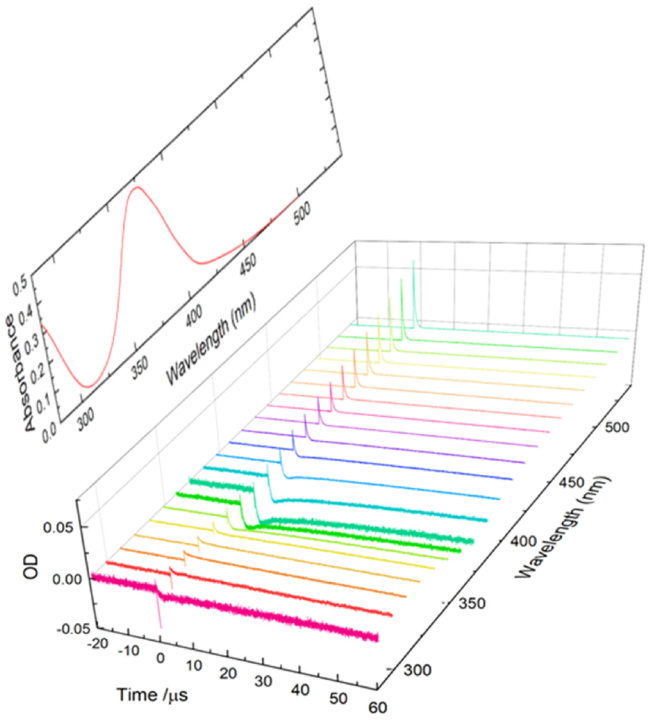

Figure 1. Changes in optical densities simultaneously measured at 21 different wavelengths as a function of time for a 49.5 μM $K_2Cr_2O_7$ solution at pH 9.8 and 25 °C with a 15 ns electron pulse of 26.8 Gy alongside an absorption spectrum of the unirradiated solution.

•OH. The other notable feature of these curves is the e_{aq}^- decay, which can be seen as a peak in the first few microseconds after the pulse. As the measurement wavelength increases, so does the contribution from the e_{aq}^- decay as it approaches its maximum absorbance at 720 nm.

3.2. Cr(VI) + e_{aq}^-. The reaction between the hydrated electron (e_{aq}^-) and chromate solutions was studied at pH 4.0, 5.5, and 9.8 at temperatures up to 325 °C. An example decay of the e_{aq}^- absorption signal is shown for solutions with different Cr concentrations at 532 nm at both 25 and 250 °C in Figure 2. Each e_{aq}^- decay trace is fit with a double exponential decay function, where one decay represents the dose-dependent contribution of the sapphire windows to the overall observed optical absorption, and the other, much larger, exponential represents the pseudo-first-order rate coefficient for the e_{aq}^- decay. The long-term sapphire window absorbance always contributed less than 1 mOD to the overall observed change in optical density. From the timescale of these plots, it can be seen that the rate is greatly increased with temperature. The pseudo-first-order rate coefficients are plotted as a function of the Cr(VI) concentration to obtain the second-order rate coefficients, as shown in Supporting Information (SI) Figure S1 for pH 4.0 solutions with 11.6 Gy and 34.7 Gy electron pulses at 75.3 °C. The rate coefficients given in the paper are shown extrapolated to zero ionic strength. At high chromium ion concentrations and high temperatures, the ionic strength correction becomes statistically significant. Figures S2 and S3 show the effect of this correction on pH 5.5 solutions with 27.7 Gy electron pulses at 25 and 249.3 °C, respectively.

The change in Cr(VI) speciation as a function of pH and temperature according to the chromic acid ionization in eqs 2 and 3 is shown in Figures S4–S6. The speciation between $HCrO_4^-$ and CrO_4^{2-} in these solutions was determined, and the individual second-order rate coefficients for each species reacting with e_{aq}^- were isolated by assuming no interconversion between chromate and bichromate over the timescale of their reactions with the hydrated electron.

The Arrhenius plots of the natural logarithm of the fitted second-order rate coefficients vs $1000/T$, where T is the temperature in Kelvin, are given in Figure 3. Both the reactions with chromate (CrO_4^{2-}) and bichromate ($HCrO_4^-$) show linear Arrhenius behavior until at least 225 °C, regardless of the solution pH. The room-temperature rate coefficients and Arrhenius parameters for all the measured reactions are tabulated in Table 1. The activation energies are within the combined experimental uncertainties for the two chromium(VI) species. Based on their rate coefficients and calculated reaction radii, these reactions with the hydrated electron are likely to be diffusion controlled and occur via long-range electron transfer processes.[29] The rate coefficients for $HCrO_4^-$

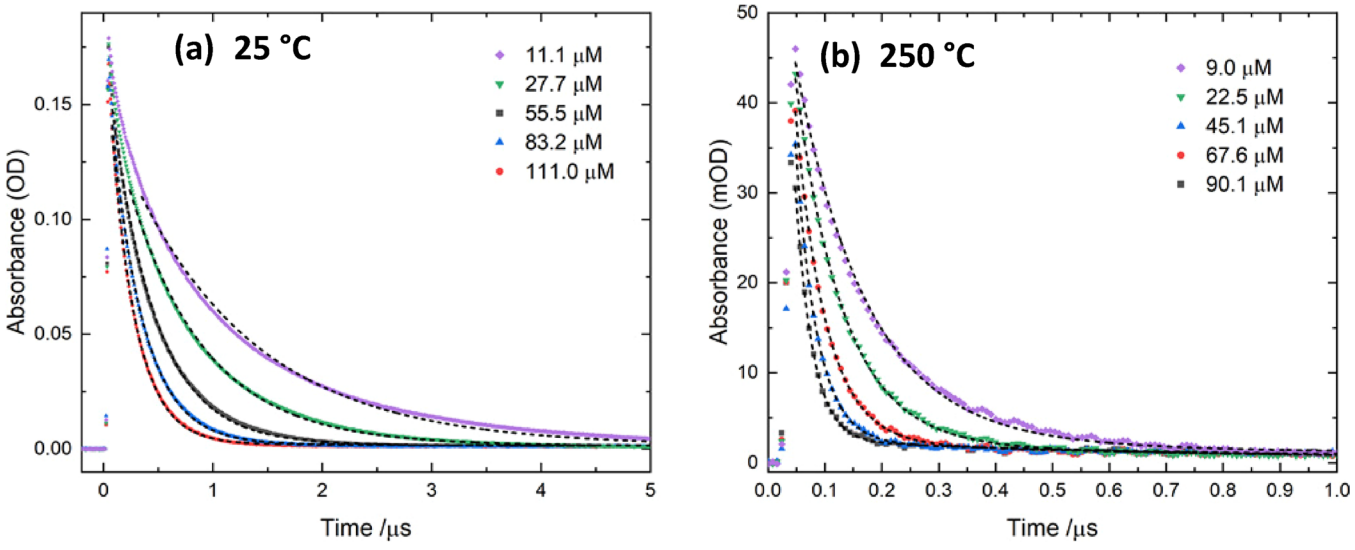

Figure 2. Decay of e_{aq}^- at 532 nm at (a) 25 °C and (b) 250 °C after a 29.2 Gy pulse in aqueous solutions of Cr(VI) with room temperature pH 5.5. Dashed black lines represent the results of system-wide fits to double exponential decays.

https://doi.org/10.1021/acsomega.2c04807
ACS Omega 2022, 7, 39071−39077

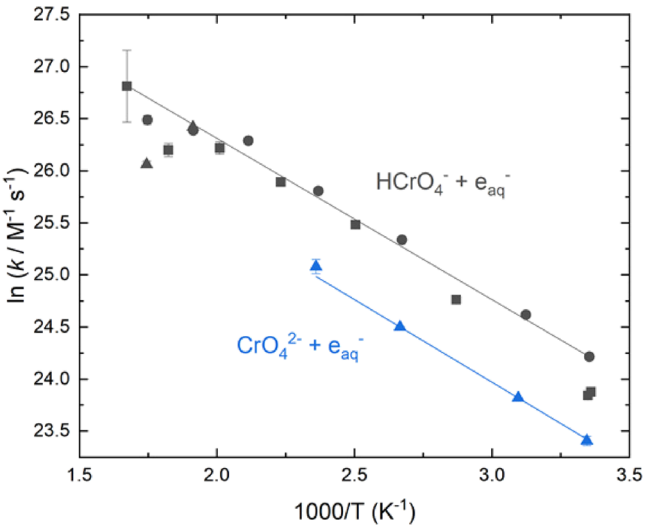

Figure 3. Arrhenius plots of the natural logarithm of the second-order rate coefficient for the reactions between e_{aq}^- and the Cr(VI) species, corrected for ionic strength. $HCrO_4^-$ (black) or CrO_4^{2-} (blue) at temperatures up to 325 °C. The symbols represent the room-temperature pH of the solution from which the rate coefficient was obtained: (square) pH 4.0, (circle) pH 5.5, and (triangle) pH 9.8.

and CrO_4^{2-} reacting with e_{aq}^- have been reported previously using electron pulse radiolysis at 25 °C; however, it is difficult to compare directly with these results as most studies do not report the uncertainties, the exact solution conditions, and/or whether or not they corrected for ionic strength.[19−23] Baxendale et al. and Peled and Czapski both found that $k(CrO_4^{2-} + e_{aq}^-) = 1.8 \times 10^{10}$ M^{-1} s^{-1}, which is slightly faster than the value measured in this work.[19,20] More recently, Lai and Freeman measured the Arrhenius behavior of CrO_4^{2-} + e_{aq}^- up to 80 °C and found that $k(CrO_4^{2-} + e_{aq}^-) = 1.7 \times 10^{10}$ M^{-1} s^{-1} at 25 °C, with an activation energy of E_A = 16 kJ/mol and pre-exponential factor of $A = 10^{13}$ M^{-1} s^{-1}.[22] Again, the reported rate is faster than that found in this work; however, the Li_2CrO_4 solutions employed by Lai and Freeman would have been ∼pH 8, affording ∼6% speciation to $HCrO_4^-$, which would increase their measured rate relative to a solution of pure CrO_4^{2-}. In addition, applying ionic strength corrections would lower their reported rate. Thomas, Gordon, and Hart report $k = 3.3 \times 10^{10}$ M^{-1} s^{-1} at pH ∼7 and $k = 5.4 \times 10^{10}$ M^{-1} s^{-1} at pH ∼13 with 1 mM methanol.[23] According to Cr(VI) speciation calculations, the pH 7 results would correspond to a solution of 95% $HCrO_4^-$, which makes this value identical to within the uncertainty with the value obtained in this work. The pH 13 result, corresponding to a solution of 100% CrO_4^{2-}, gives a rate faster than that found in this and other studies and is likely in error.[19−22]

3.3. Cr(VI) + H•. The reaction between the hydrogen atom (H•) and bichromate solutions was studied at pH 4.0 and 5.5 at temperatures up to 250 °C. The decay of $HCrO_4^-$ from its baseline optical absorption maximum was studied at 348 nm. An example of the $HCrO_4^-$ absorption signal bleach and recovery at 348 nm is shown for solutions with different chromium concentrations at both 25 and 250 °C in Figure 4. After a rapid bleach, as some of $HCrO_4^-$ reacts with H• and e_{aq}^-, the $HCrO_4^-$ solution recovered partially toward its baseline value due to the back reaction of Cr(V) + •OH. This mechanism was confirmed by adding methanol to the solutions to scavenge •OH, in which case the recovery toward the initial $HCrO_4^-$ absorption was not seen, as shown in Figure S7. Each optical density trace is fit by first assuming the following temperature-dependent yields of water radiolysis products:[30−32]

$$G(H^\bullet + e_{aq}^-) = 2.868 + 7.573 \times 10^{-3}\, t + 2.50 \times 10^{-6}\, t^2 \quad (6)$$

$$G(e_{aq}^-) = 2.4297 + 3.829 \times 10^{-3}\, t + 8.3656 \times 10^{-6}\, t^2 - 4.3396 \times 10^{-8}\, t^3 \quad (7)$$

$$G(H^\bullet) = G(H^\bullet + e_{aq}^-) - G(e_{aq}^-) \quad (8)$$

$$G(H_2) = 0.419 + 8.721 \times 10^{-4}\, t - 4.971 \times 10^{-6}\, t^2 + 1.508 \times 10^{-8}\, t^3 \quad (9)$$

$$G(^\bullet OH) = 2G(H_2) + G(H^\bullet + e_{aq}^-) - 2G(H_2O_2) \quad (10)$$

$$G(H_2O_2) = 0.752 - 1.620 \times 10^{-3}\, t \quad (11)$$

where t is the temperature in °C, the yields (G values) of the species are in units of molecules/100 eV, and the absorbed doses were determined by dosimetry measurements. The measured change in optical density is fit with the system of chemical reactions for water radiolysis assembled by Elliot and Bartels,[31] including competitive reactions such as the bimolecular combinations of H• and •OH, supplemented with the additional reactions of the Cr(VI) ions being studied:

$$HCrO_4^- + e_{aq}^- \rightarrow Cr(V), \quad k_{12} = 5.913 \times 10^{12} \exp(-1548.51/T) \quad (12)$$

$$HCrO_4^- + H^\bullet \rightarrow Cr(V), \quad k_{13} \quad (13)$$

$$Cr(V) + {}^\bullet OH \rightarrow Cr(VI), \quad k_{14} \quad (14)$$

where the rate constant for k_{12} was determined in Section 3.2, and k_{13} and k_{14} are fitted parameters along with the temperature-dependent extinction coefficients for the Cr(VI) species. The change in optical density is given by the sum of contributions from chromium and water radiolysis species. The extinction coefficients for water radiolysis products e_{aq}^- and •OH were also fitted for a given temperature with initial guesses based on literature values.[33,34]

Table 1. Summary of the Rate Coefficients and Arrhenius Parameters for the Reactions between Cr(VI) Ions and Water Radiolysis Products in Aqueous Solutions

reaction	solution pH (25 °C)	k_0 (M^{-1} s^{-1}) (25 °C)	activation energy, E_a (kJ mol^{-1})	pre-exponential factor, A(M^{-1} s^{-1})
$HCrO_4^- + e_{aq}^-$	4.0, 5.5, 9.8	$(3.28 \pm 0.58) \times 10^{10}$	12.88 ± 0.56	$(5.91 \pm 0.10) \times 10^{12}$
$CrO_4^{2-} + e_{aq}^-$	9.8	$(1.47 \pm 0.10) \times 10^{10}$	13.19 ± 0.12	$(3.00 \pm 0.13) \times 10^{12}$
$HCrO_4^- + H^\bullet$	4.0, 5.5	$(1.19 \pm 0.17) \times 10^{10}$	12.98 ± 0.29	$(2.24 \pm 0.17) \times 10^{12}$
Cr(V) + •OH	4.0, 5.5	$(4.80 \pm 0.52) \times 10^{9}$	7.03 ± 0.22	$(8.17 \pm 0.54) \times 10^{10}$

https://doi.org/10.1021/acsomega.2c04807
ACS Omega 2022, 7, 39071−39077

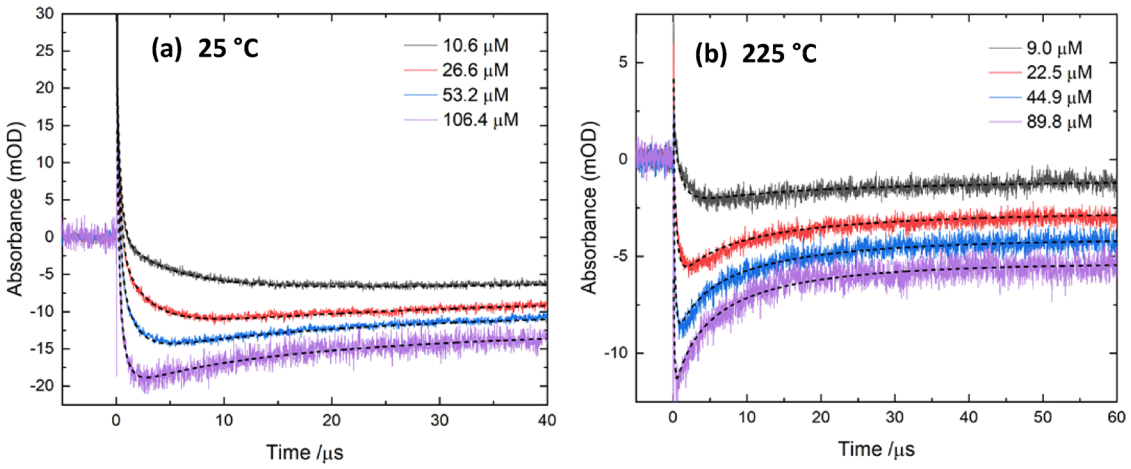

Figure 4. Bleach and subsequent recovery of the $HCrO_4^-$ optical absorbance at 348 nm at (a) 25 °C, and (b) 225 °C after a 26.6 Gy electron pulse in aqueous solutions with room-temperature pH 4.0. Dashed black lines represent the system-wide optical absorption fit results from using eqs 6−14.

Figure 5 shows the Arrhenius plots of the natural logarithm of the fitted second-order rate coefficients vs $1/T$. The room-temperature rate coefficient, $k_{13} = (1.19 \pm 0.17) \times 10^{10}$ M^{-1} s^{-1}, and its associated Arrhenius parameters are listed in Table 1. Cr(VI) + H• was also measured in solutions at pH 1.1 up to 80 °C, but since the water radiolysis G-values increase at pH < 4 and these values are not known as a function of temperature,[35] the fitting function could not be used for these solutions. Instead, a single exponential function was fit to the initial $HCrO_4^-$ decay kinetics, which resulted in the rate coefficients plotted in red in Figure 5. These values do not completely agree with those determined at pH 4.0 and 5.5 because of the added uncertainty from fitting just the $HCrO_4^-$ decay and because at pH 1.1 there will be some speciation to H_2CrO_4. If H_2CrO_4 does not react significantly with the H• atom, such that the entire measured rate coefficient at pH 1.1 comes from $HCrO_4^-$ + H•, then the pK_a value for H_2CrO_4 required to move the measured rate coefficient in line with the values determined at pH 4.0 and 5.5 can be calculated at each temperature. Using this approach, a pK_a of 0.022 ± 0.421 was determined for chromic acid at 25 °C, which falls within the range of values from −1.0 to 1.6 reported in the literature.[11−13] Using a van't Hoff fit of the pK_a values determined at each temperature, the enthalpy and entropy of the chromic acid dissociation reaction were found to be $\Delta_r H = -16.5 \pm 3.1$ kJ/mol and $\Delta_r S = -57.8 \pm 9.2$ J/K.

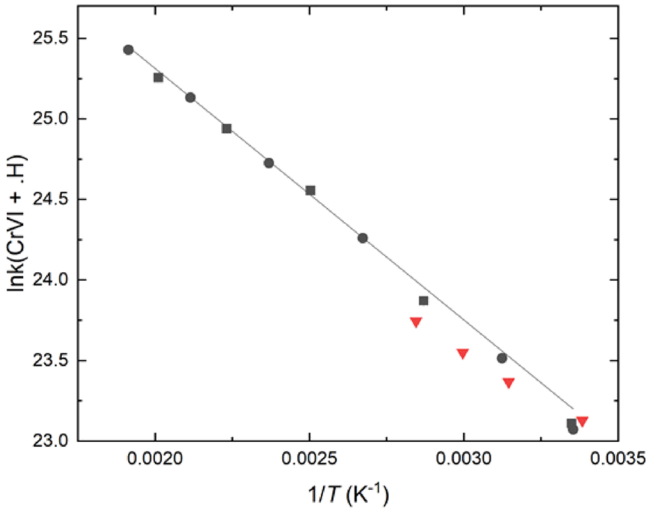

Figure 5. Arrhenius plots of the natural logarithm of the second-order rate coefficient for the reactions between the H• atom and $HCrO_4^-$ at temperatures up to 275 °C. The symbols represent the room-temperature pH of the solution from which the rate coefficients were obtained: (square) pH 4.0, (circle) pH 5.5, and (red inverted triangle) pH 1.1.

The rate coefficient for $HCrO_4^-$ + H• has been reported previously at 25 °C.[5,24,25] Hayon and Moreau used steady-state irradiations and competition kinetics with ethanol at neutral pH to obtain rate coefficients of $k = 0.6-2.6 \times 10^{10}$ M^{-1} s^{-1} for this reaction.[24] Sharpe and Sehested measured an approximate value of $k(HCrO_4^- + H^\bullet) = 1.5 \times 10^{10}$ M^{-1} s^{-1}, which may be within the experimental uncertainty of the value obtained in this work.[25] Al-Sheikhly and McLaughlin reported $k = 2.3 \times 10^{10}$ M^{-1} s^{-1} at pH 0.4;[5] however, at this pH, a significant portion of Cr(VI) may be present as H_2CrO_4.

3.4. Cr(V) + •OH. For the pH 4.0 and 5.5 solutions, the rate coefficients for Cr(V) + •OH were also obtained from the fits used for Cr(VI) + H• as described in the previous section. Figure 6 shows the Arrhenius plot resulting from fitting the Cr(VI) optical density recovery at 348 nm for this reaction. The room-temperature rate coefficient, k_{14}(Cr(V) + •OH) = $(4.80 \pm 0.52) \times 10^9$ M^{-1} s^{-1}, and the corresponding Arrhenius parameters are given in Table 1. The pre-exponential factor for this reaction is significantly lower than that seen for the reactions between Cr(VI) and the primary radiolysis products of water.

The rate coefficient for Cr(V) + •OH has been reported previously in pH 1 solution at 25 °C by Sharpe and Sehested as $k = (1.5 \pm 0.5) \times 10^9$ M^{-1} s^{-1}.[25] This reaction has also been described at room temperature in basic solution where Baxendale et al. found that k(Cr(V) + •OH) = 5×10^{10} M^{-1} s^{-1}, based on the relative absorptions of CrO_4^{2-} and the Cr(V) transient at 365 nm.[19] The result from this work at intermediate pH falls between those at high and low pH previously reported. This rate coefficient determines how much of the Cr(V) outcompetes •OH combining with itself, thus affecting the amount of $HCrO_4^-$ recovered after the pulse. At pH 1, only 20% of the Cr(V) was seen to react,[25] where in basic solutions, CrO_4^{2-} was entirely recovered.[19] The large

https://doi.org/10.1021/acsomega.2c04807
ACS Omega 2022, 7, 39071−39077

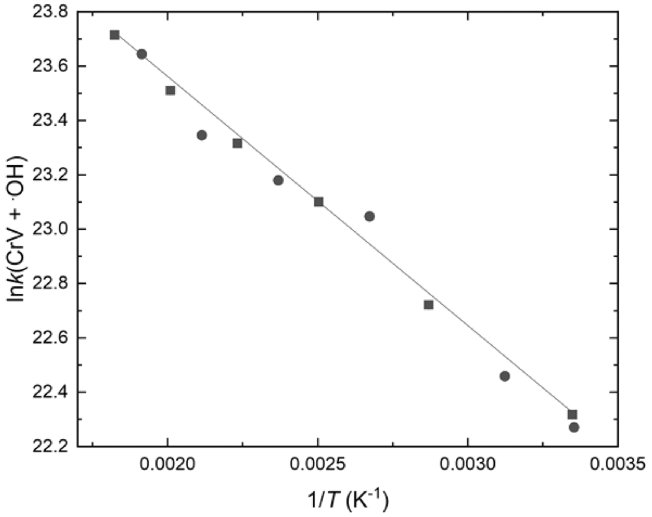

Figure 6. Arrhenius plots of the natural logarithm of the second-order rate constant for the reactions between Cr(V) and •OH at temperatures up to 275 °C. The symbols represent the room-temperature pH of the solution from which the rate coefficients were obtained: (square) pH 4.0; (circle) pH 5.5.

variation in this rate coefficient with pH between the different studies is not fully understood. Sharpe and Sehested speculated that this effect may be due to spectral changes associated with rapid protonation reactions.[25]

The change in the absorbance spectrum for a 55.5 μM $K_2Cr_2O_7$ solution at pH 5.5 from 0 to 10 μs after a 29.2 Gy electron pulse at 25 °C is shown in Figure S8. By subtracting the absorbance due to the concentration of $HCrO_4^-$ lost assuming that $G(H^\bullet + e_{aq}^-) = 3.059$ molecules/100 eV, one can see that the Cr(V) product has an absorbance maximum around ~320 nm. The hypochromate ion, CrO_4^{3-}, is predicted to be the primary Cr(V) product in alkaline solutions and is known to absorb around 355 nm.[36] The species formed under acidic solutions is not currently known but may be a protonated form of the basic product.

4. CONCLUSIONS

The rate coefficients and Arrhenius parameters for the major reactions of aqueous Cr(VI) ions under irradiation have been measured for the first time to high temperatures. All measured rate coefficients increased exponentially with temperature, and the activation energies for the reactions of $HCrO_4^-$ and CrO_4^{2-} agreed within the experimental uncertainties. The reduction reactions of Cr(VI) to Cr(V) by the e_{aq}^- or H• atom are significantly reversed by the back reaction of the product Cr(V) with the •OH radical, and the extent of this oxidation reaction has a strong dependence on pH.

Overall, the new kinetic data measured in this work give a much better understanding of the speciation of chromium in aqueous solution under irradiation and at high temperatures. More studies on the radiation chemistry reactions of the other oxidation states of Cr to high temperatures are required to build a complete model of its behavior and thus be able to predict and control Cr speciation in aqueous solution under irradiation for applications such as corrosion product transport in nuclear reactor coolant. The results from this work do support the idea that Cr(VI) can be reduced under irradiation for the proposed radiolytic reduction of Cr(VI) to Cr(III) for environmental release; however, the back reaction between Cr(V) and the •OH radical also has important implications for this application. This reaction suggests that a scavenger for the •OH radical would need to be included in the system to efficiently achieve a complete conversion. For the same reasons, this observation also complicates the proposed use of aqueous Cr(VI) solution as a chemical dosimeter, as the loss of Cr(VI) would not simply be linear with the absorbed dose.

■ ASSOCIATED CONTENT

Supporting Information

The Supporting Information is available free of charge at https://pubs.acs.org/doi/10.1021/acsomega.2c04807.

Linear fits of pseudo-first-order rate coefficients to obtain second-order rate coefficients, concentration of Cr(VI) species as a function of temperature and pH, change in the $HCrO_4^-$ optical absorbance with 10 mM MeOH as an •OH scavenger, optical absorption of the full spectrum, and subtracted Cr(V) transient species formed in an irradiated $K_2Cr_2O_7$ solution (PDF)

■ AUTHOR INFORMATION

Corresponding Authors

Jacy K. Conrad − *Center for Radiation Chemistry Research, Idaho National Laboratory, Idaho Falls, Idaho 83415, United States;* orcid.org/0000-0002-0745-588X; Email: jacy.conrad@inl.gov

David M. Bartels − *Notre Dame Radiation Laboratory, University of Notre Dame, Notre Dame, Indiana 46556, United States;* orcid.org/0000-0003-0552-3110; Email: David.M.Bartels.5@nd.edu

Author

Aliaksandra Lisouskaya − *Notre Dame Radiation Laboratory, University of Notre Dame, Notre Dame, Indiana 46556, United States;* orcid.org/0000-0001-7556-8977

Complete contact information is available at: https://pubs.acs.org/10.1021/acsomega.2c04807

Notes

The authors declare no competing financial interest.

■ ACKNOWLEDGMENTS

This work was supported through the INL Laboratory Research & Development (LDRD) Program under DOE Idaho Operations Office Contract DE-AC07-05ID14517. The NDRL is supported by the Division of Chemical Sciences, Geosciences and Biosciences, Basic Energy Sciences, Office of Science, US-DOE through Award No. DE-FC02-04ER15533. This is manuscript #5369 of the Notre Dame Radiation Laboratory.

■ REFERENCES

(1) Coetzee, J. J.; Bansal, N.; Chirwa, E. M. N. Chromium in Environment, Its Toxic Effect from Chromite-Mining and Ferro-chrome Industries, and Its Possible Bioremediation. *Exposure Health* **2020**, *12*, 51−62.

(2) Comley, G. C. W. The significance of corrosion products in water-reactor coolant circuits. *Prog. Nucl. Energy* **1985**, *16*, 41−72.

(3) Alrehaily, L. M.; Joseph, J. M.; Musa, A. Y.; Guzonas, D. A.; Wren, J. C. Gamma-radiation induced formation of chromium oxide nanoparticles from dissolved dichromate. *Phys. Chem. Chem. Phys.* **2013**, *15*, 98−107.

(4) Dehghani, M. H.; Heibati, B.; Asadi, A.; Tyagi, I.; Agarwal, S.; Gupta, V. K. Reduction of noxious Cr(VI) ion to Cr(III) ion in aqueous solutions using H_2O_2 and UV/H_2O_2 systems. *J. Ind. Eng. Chem.* **2016**, *33*, 197−200.
(5) Al-Sheikhly, M.; McLaughlin, W. L. The mechanisms of the reduction reactions of Cr(VI) in the radiolysis of acidic potassium and silver dichromate solutions in the presence or absence of acetic acid. *Radiat. Phys. Chem.* **1991**, *38*, 203−211.
(6) Anderson, A. R.; Farhataziz. ^{60}Co gamma radiolysis of potassium dichromate in acid solution. *Trans. Faraday Soc.* **1963**, *59*, 1299.
(7) Buxton, G. V.; Djouider, F. Use of the dichromate solution as a dosimeter for high dose and high dose rate. *Radiat. Phys. Chem.* **1996**, *48*, 799−804.
(8) Sharpe, P. H. G.; Miller, A.; Bjergbakke, E. Dose rate effects in the dichromate dosimeter. *Radiat. Phys. Chem.* **1990**, *35*, 757−761.
(9) Spinks, J. W. T.; Woods, R. J.*Introduction to Radiation Chemistry*; 3rd ed.; John Wiley & Sons Inc.: Canada, 1990.
(10) Buxton, G. V.; Greenstock, C. L.; Helman, W. P.; Ross, A. B. Critical review of rate constants for reactions of hydrated electrons, hydrogen atoms and hydroxyl radicals (•OH/•O-) in aqueous solution. *J. Phys. Chem. Ref. Data* **1988**, *17*, 513−886.
(11) Palmer, D. A.; Wesolowski, D.; Mesmer, R. E. A potentiometric investigation of the hydrolysis of chromate(VI) ion in NaCl media to 175 °C. *J. Solution Chem.* **1987**, *16*, 443−463.
(12) Bailey, N.; Carrington, A.; Lott, K. A. K.; Symons, M. C. R. Structure and reactivity of the oxyanions of transition metals 8. Acidities and spectra of protonated oxyanions. *J. Chem. Soc.* **1960**, 290−297.
(13) Chlistunoff, J. B.; Johnston, K. P. UV-vis spectroscopic determination of the dissociation constant of bichromate from 160 to 400 degrees C. *J. Phys. Chem. B* **1998**, *102*, 3993−4003.
(14) Szabó, M.; Kalmár, J.; Ditrói, T.; Bellér, G.; Lente, G.; Simic, N.; Fábián, I. Equilibria and kinetics of chromium(VI) speciation in aqueous solution - A comprehensive study from pH 2 to 11. *Inorg. Chim. Acta* **2018**, *472*, 295−301.
(15) Wagman, D. D.; Evans, W. H.; Parker, V. B.; Schumm, R. H.; Halow, I.; Bailey, S. M.; Churney, K. L.; Nuttall, R. L. The NBS tables of chemical thermodynamic properties. Selected values for inorganic and C1 and C2 organic substances in SI units. *J. Phys. Chem. Ref. Data* **1982**, *11*, 2.
(16) Baes, C. F.; Mesmer, R. E.*The Hydrolysis of Cations*; Wiley-Interscience: New York, 1976. https://onlinelibrary.wiley.com/doi/abs/10.1002/bbpc.19770810252
(17) Brown, P. L.; Ekberg, C.*Hydrolysis of Metal Ions*; Wiley-VCH Verlag GmbH & Co.: Weinheim, Germany, 2016. https://www.wiley.com/en-us/Hydrolysis+of+Metal+Ions-p-9783527330102
(18) Johnson, J. W.; Oelkers, E. H.; Helgeson, H. C. SUPCRT92 - A software package for calculating the standard molal thermodynamic properties of minerals, gases, aqueous species, and reactions from 1 bar to 5000 bar and 0 °C to 1000 °C. *Comput. Geosci.* **1992**, *18*, 899−947.
(19) Baxendale, J. H.; Fielden, E. M. The Pulse Radiolysis of Aqueous Solutions of Some Inorganic Compounds. *Proc. R. Soc. London, Ser. A* **1965**, *286*, 320−336.
(20) Peled, E.; Czapski, G. Studies on the Molecular Hydrogen Formation (GH_2) in the Radiation Chemistry of Aqueous Solutions. *J. Phys. Chem.* **1970**, *74*, 2903−2911.
(21) Pikaev, A. K.; Zansokhova, A. A.; Kabakchi, S. A. Kinetics of reactions and yield of hydrogen ions from pulse radiolysis of aqueous solutions of potassium chromate. *Radiat. Phys. Chem.* **1980**, *16*, 125−131.
(22) Lai, C. C.; Freeman, G. R. Solvent effects on the reactivity of solvated electrons with charged solutes in methanol/water and ethanol/water mixed solvents. *J. Phys. Chem.* **1990**, *94*, 4891−4896.
(23) Thomas, J. K.; Gordon, S.; Hart, E. J. The Rates of Reaction of the Hydrated Electron in Aqueous Inorganic Solutions. *J. Phys. Chem.* **1964**, *68*, 1524−1527.
(24) Hayon, E.; Moreau, M. Réactivité des atomes H avec quelques composés organiques et minéraux en solutions aqueuses. *J. Chim. Phys.* **1965**, *62*, 391−391.
(25) Sharpe, P. H. G.; Sehested, K. The dichromate dosimeter: A pulse-radiolysis study. *Radiat. Phys. Chem.* **1989**, *34*, 763−768.
(26) Anbar, M.; Hart, E. J. Reactivity of metal ions and some oxy anions toward hydrated electrons. *J. Phys. Chem.* **1965**, *69*, 973.
(27) Lisovskaya, A.; Kanjana, K.; Bartels, D. M. One-electron redox kinetics of aqueous transition metal couples $Zn^{2+/+}$, $Co^{2+/+}$, and $Ni^{2+/+}$ using pulse radiolysis. *Phys. Chem. Chem. Phys.* **2020**, *22*, 19046−19058.
(28) Takahashi, K.; Cline, J. A.; Bartels, D. M.; Jonah, C. D. Design of an optical cell for pulse radiolysis of supercritical water. *Rev. Sci. Instrum.* **2000**, *71*, 3345−3350.
(29) Schmidt, K. H.; Han, P.; Bartels, D. M. Radiolytic yields of the hydrated electron from transient conductivity - Improved calculation of the hydrated electron-diffusion coefficient and analysis of some diffusion-limited e_{aq}^- reaction-rates. *J. Phys. Chem.* **1995**, *99*, 10530−10539.
(30) Sterniczuk, M.; Yakabuskie, P. A.; Wren, J. C.; Jacob, J. A.; Bartels, D. M. Low LET radiolysis escape yields for reducing radicals and H_2 in pressurized high temperature water. *Radiat. Phys. Chem.* **2016**, *121*, 35−42.
(31) Elliot, A. J.; Bartels, D. M.*The Reaction Set, Rate Constants and G-Values for the Simulation of the Radiolysis of Light Water Over the Range 20° to 350°C Based on Information*; Available in 2008; AECL Nuclear Platform Research and Development, 2009. https://inis.iaea.org/search/search.aspx?orig_q=RN:41057263
(32) Sterniczuk, M.; Bartels, D. M. Source of Molecular Hydrogen in High-Temperature Water Radiolysis. *J. Phys. Chem. A* **2016**, *120*, 200−209.
(33) Janik, I.; Bartels, D. M.; Jonah, C. D. Hydroxyl radical self-recombination reaction and absorption spectrum in water up to 350 degrees C. *J. Phys. Chem. A* **2007**, *111*, 1835−1843.
(34) Hare, P. M.; Price, E. A.; Stanisky, C. M.; Janik, I.; Bartels, D. M. Solvated Electron Extinction Coefficient and Oscillator Strength in High Temperature Water. *J. Phys. Chem. A* **2010**, *114*, 1766−1775.
(35) Ferradini, C.; Jay-Gerin, J.-P. The Effect of pH on Water Radiolysis: A Still Open Question - A Minireview. *Res. Chem. Intermed.* **2000**, *26*, 549−565.
(36) Bailey, N.; Symons, M. C. R. Structure and Reactivity of the Oxyanions of Transition Metals. Part III: The Hypochromate Ion. *J. Chem. Soc* **1957**, 203−207.

https://doi.org/10.1021/acsomega.2c04807
ACS Omega 2022, 7, 39071−39077